



HAL
open science

Circuit-level analysis identifies target genes of sex steroids in ewe seasonal breeding

Didier Lomet, Xavier Druart, David Hazlerigg, Massimiliano Beltramo,
Hugues Dardente

► **To cite this version:**

Didier Lomet, Xavier Druart, David Hazlerigg, Massimiliano Beltramo, Hugues Dardente. Circuit-level analysis identifies target genes of sex steroids in ewe seasonal breeding. *Molecular and Cellular Endocrinology*, 2020, 512, pp.1-10. 10.1016/j.mce.2020.110825 . hal-03115205

HAL Id: hal-03115205

<https://hal.science/hal-03115205>

Submitted on 22 Aug 2022

HAL is a multi-disciplinary open access archive for the deposit and dissemination of scientific research documents, whether they are published or not. The documents may come from teaching and research institutions in France or abroad, or from public or private research centers.

L'archive ouverte pluridisciplinaire **HAL**, est destinée au dépôt et à la diffusion de documents scientifiques de niveau recherche, publiés ou non, émanant des établissements d'enseignement et de recherche français ou étrangers, des laboratoires publics ou privés.



Distributed under a Creative Commons Attribution - NonCommercial 4.0 International License

1 Circuit-level analysis identifies target genes of sex steroids in ewe seasonal breeding.

2
3 Didier Lomet¹, Xavier Druart¹, David Hazlerigg², Massimiliano Beltramo¹ and Hugues
4 Dardente^{1,3*}

5 ¹PRC, INRAE, CNRS, IFCE, Université de Tours, 37380 Nouzilly, France

6 ²Department of Arctic and Marine Biology, University of Tromsø, 9037 Tromsø, Norway

7 ³Lead Contact

8 *Correspondence: hugues.dardente@inrae.fr

9
10 **Abstract**

11
12 Thyroid hormone (TH) and estradiol (E2) direct seasonal switches in ovine reproductive
13 physiology. In sheep, as in other mammals and birds, control of thyrotropin (TSH) production
14 by the *pars tuberalis* (PT) links photoperiod responsiveness to seasonal breeding. PT-derived
15 TSH governs opposite seasonal patterns of the TH deiodinases *Dio2/Dio3* expression in
16 tanycytes of the neighboring medio-basal hypothalamus (MBH), which explain the key role of
17 TH. We recently used RNA-Seq to identify seasonal markers in the MBH and define the impact
18 of TH. This impact was found to be quite limited, in terms of number of target genes, and very
19 restricted with regards to neuroanatomical location, as TH specifically impacts genes expressed
20 in tanycytes and hypothalamus, not in the PT. Here we address the impact of E2 on these
21 seasonal markers, which are specifically expressed in either PT, tanycytes or hypothalamus.
22 We also investigate if progesterone (P4) may be involved in timing the seasonal transition to
23 anestrus. Our analysis provides circuit-level insights into the impact of sex steroids on the ewe
24 seasonal breeding cycle. First, seasonal gene expression in the PT is independent of the sex
25 steroid status. The fact that seasonal gene expression in the PT is also TH-independent
26 strengthens the view that the PT is a circannual timer. Second, select tanycytic markers display

27 some level of responsiveness to E2 and P4, which indicates another potential level of feedback
28 control by sex steroids. Third, *Kiss1* neurons of the arcuate nucleus are responsive to both TH
29 and E2, which places them at the crossroads of photoperiodic transduction pathway and sex
30 steroid feedback. This provides strong support to the concept that these *Kiss1* neurons are
31 pivotal to the long-recognized “seasonal switch in the ability of E2 to exert negative feedback”,
32 which drives seasonal breeding.

33

34 **Keywords**

35 Biological rhythms, breeding, circannual clock, estradiol, GnRH, kisspeptin, Kiss1, melatonin,
36 *pars tuberalis*, photoperiod, pituitary, progesterone, RFRP3, seasonality, sheep, tanycytes,
37 thyrotropin.

38

39 **Declaration of interest:** none.

40

41 **Abbreviations**

42 DEG: differentially expressed genes; E2: estradiol; IdF: Ile-de-France breed; ISH: *in situ*
43 hybridization; LH: luteinizing hormone; LP: long photoperiod; MBH: medio-basal hypothalamus;
44 OVX: ovariectomized; P4: progesterone; PGR: P4 receptor; PT: *pars tuberalis* of the pituitary;
45 RIA: radioimmunoassay; Rom: Romanov breed; SCN: suprachiasmatic nucleus of the
46 hypothalamus; SP: short photoperiod; TH: thyroid hormones; T3: triiodothyronine; TRH:
47 thyrotropin-releasing hormone; TSH: thyrotropin; ZT: zeitgeber time.

48

49

50

51

52 **Introduction**

53 The *pars tuberalis* (PT) of the pituitary is the key target tissue of melatonin for the control of
54 seasonal breeding (Dardente et al 2014; Dardente et al 2019a; Wood and Loudon 2018). In the PT,
55 a short duration of nightly melatonin production, typical of longer spring/summer days, triggers
56 the expression of *Tshb* through TEF/EYA3/SIX1, a triad of transcription factors and co-activators
57 (Dardente et al 2010). This specific PT-derived TSH acts on neighboring tanycytes, which line the
58 walls of the third ventricle, to induce the expression of deiodinase II (*Dio2*) and repress expression
59 of *Dio3*, leading to increased local T3 production (Nakao et al 2008; Hanon et al 2008; Ono et al
60 2008). This opposite photoperiodic control over *Dio2* and *Dio3* is responsible for the tight seasonal
61 control of T3 levels within the medio-basal hypothalamus (MBH), which governs physiological
62 switches in the annual breeding cycle of multiple species, including sheep (Karsch et al 1995;
63 Dardente 2012).

64
65 Our recent RNAseq analysis of the MBH in ovariectomized estradiol-implanted (OVX+E2) ewes
66 revealed that ~10% of protein-coding genes display differential expression levels between May
67 and November, which illustrates the potent transcriptome-wide impact of photoperiod (Lomet et
68 al 2018; Dardente & Lomet 2018). We validated seasonal changes in the expression level for the
69 top ~30 differentially expressed genes (DEG). Most DEG were found either in the PT (e.g. *Tshb*,
70 *Fam150b*, *Vmo1*, *Ezh2*, *Suv39H2*, *Vcan*, *Aa-Nat* and *Chga*) or in tanycytes of the beta subtypes,
71 located at the bottom of the third ventricle (e.g. *Dio2*, *Tmem252*, *Shh*, *Slc01c1*, *Dct* and *NpSRI*).

72
73 *Kiss1* and *Npvf* (encoding the RF-amide peptides KISS1 and RFRP3), which are expressed by
74 discrete clusters of neurons within the MBH parenchyma (Smith 2009; Lomet et al 2018;
75 Angelopoulou et al 2019), were also identified as DEG. The MBH is key to the central control of
76 breeding and appears to host the long sought-after GnRH pulse generator. There is now strong

77 evidence that KNDy (KISS1/NeurokininB/Dynorphin) neurons located in the arcuate nucleus are
78 the GnRH pulse generator (Lehman et al 2010; Han et al 2015; Moore et al 2018; Herbison 2018).
79 We found that *Kiss1* displays a marked (~10-fold) seasonal rhythm in expression in OVX+E2
80 ewes, leading to heightened expression during short winter days (Lomet et al 2018), consistent
81 with prior findings (Smith et al 2008 ; Wagner et al 2008 ; Urias-Castro et al 2019). In intact ewes,
82 this increase in KISS1 presumably leads to enhanced GnRH secretion, which triggers breeding
83 (Messenger et al 2005; Caraty et al 2007; Caraty et al 2013). Furthermore, in sheep as in other
84 mammals a vast majority of KNDy neurons express receptors for E2 and P4 (ERa and PGR,
85 respectively ; Goubillon et al 2000 ; Dufourny and Skinner 2002 ; Franceschini et al 2006 ; Smith
86 et al 2007 ; Foradori et al 2002 ; Campbell et al 2017 ; Chen et al 2017), which confers them direct
87 responsiveness to sex steroid feedback. This is highly relevant since the current model for the
88 photoperiodic control of seasonal breeding, established in the early 80's (Legan et al 1977 ; Karsch
89 et al 1984; Goodman & Inskeep, 2015), emphasizes the role of "a seasonal switch in the ability of
90 E2 to inhibit the GnRH pulse generator" as the key event responsible for timely onset and offset
91 of breeding. Indeed, OVX+E2 ewes display overt seasonal differences in the frequency and
92 amplitude of GnRH/LH pulses, which are lost in OVX ewes (Karsch et al 1993). The neural
93 mechanism(s) driving the seasonal switch in the ability of E2 to exert negative feedback remain
94 unclear even though the MBH appears to be the key neural site (Blache et al 1991 ; Caraty et al
95 1998). Since OVX+E2 ewes undergo properly timed seasonal switches in LH/FSH, P4 appears
96 dispensable for these (Legan et al 1977). However, P4 exerts negative feed-back onto the MBH
97 during the luteal phase, which is mandatory for normal estrus cycles and fertility during the
98 breeding season (Dardente 2012 ; Goodman & Inskeep, 2015).

99
100 Even though KNDy neurons are strong contenders as a common conduit for photoperiod and sex
101 steroids towards GnRH seasonal control, we lack a comprehensive circuit-level analysis of the

102 cellular and molecular targets of E2 (and P4) responsible for the "seasonal switch". Indeed several
103 non-mutually exclusive hypotheses can be put forth: E2 may impair the photoperiodic read-out
104 mechanism in the PT, and/or modulate transduction of the signal towards tanycytes and/or
105 modulate signaling directly within the hypothalamic parenchyma. The latter possibility would
106 likely involve *Kiss1* neurons, but might also include an impact on *Npvf* neurons. Here, we used
107 our validated set of seasonal DEG to test these possibilities in ewes sampled at different times of
108 the year and under various sex steroid states (intact, OVX+E2 and OVX ewes).

109

110 **Materials & Methods**

111 **Ethics statement**

112 All experimental procedures were performed in accordance with international (directive
113 2010/63/UE) and national legislation (décret n° 2013–118) governing the ethical use of animals in
114 research (authorization n° E37–175-2 and n°A38 801). All procedures used in this work were
115 evaluated by a local ethics committee (Comité d’Ethique en Expérimentation Animale Val de
116 Loire) and approved by the Ministry of Higher Education and Research (project n°00710.02). All
117 surgeries were performed after sodium thiopental anesthesia (Nesdonal®, 1g/80kg) under constant
118 isoflurane administration (Vetflurane®) and all efforts were made to minimize suffering.
119 Following surgery, animals received an injection of antibiotics (oxytetracycline, Terramycine
120 LA®, 1ml/10kg) and an injection of a non-steroidal anti-inflammatory drug (Finadyne®, flumixin
121 megumine, 2ml/50kgs). Animals were taken care of daily throughout the experiment and killed by
122 decapitation under deep barbiturate anesthesia (Nesdonal®, 5mL). To minimize potential issues
123 linked to time-of-day fluctuation in gene expression (i.e. circadian rhythms) all animals were killed
124 in the early day (ZT1-6, with ZT0 being the time of lights on, or sunrise).

125

126

127 **Animals & Experimental procedures**

128 Experiments were conducted on adult Ile-de-France (IdF) ewes (3–5 years old; weight 60–80 kg)
129 and adult Romanov (Rom) ewes (3–5 years old; weight 60–80 kg) maintained under normal
130 husbandry at the research station of the Institut National de la Recherche Agronomique in Nouzilly
131 (PAO, INRA, 2018. Animal Physiology Experimental Facility, DOI:
132 10.15454/1.5573896321728955E12). We used either intact, ovariectomized (OVX) or
133 ovariectomized, estradiol-implanted (OVX+E2; 1cm silastic implant) ewes. This OVX+E2 model
134 normalizes the level of circulating E2, which uncovers the well-documented central seasonal shift
135 in the negative feedback action of E2 on gonadotropin secretion ([Legan et al 1977](#) ; [Karsch et al](#)
136 [1984](#); [Goodman & Inskeep, 2015](#)).

137
138 For experiment 1, *in situ* hybridization (ISH) was performed on brain sections (see next section
139 and [Lomet et al 2018](#)). For all other experiments RNA was extracted from a MBH block, which
140 comprises the PT, the median eminence, the arcuate nucleus and the dorsomedial and ventromedial
141 hypothalamic nuclei. The RNA samples were used to perform qRT-PCR; some of these samples
142 have been used in prior studies (see below and [Lomet al 2018](#), [Dardente & Lomet 2018](#)).

143
144 In experiment 1, intact IdF ewes were kept in an open barn and killed in May (non-breeding season,
145 n=6) and November (breeding season, n=6). In experiment 2, intact IdF ewes were kept in an open
146 barn and killed in November (n=6), February (when breeding stops, n=5), May (n=6) and August
147 (when breeding resumes, n=6). For experiment 3 (IdF breed), a direct comparison of expression
148 levels between May and November was performed across three distinct conditions with respect to
149 sex steroid status: intact ewes (groups from Expt 2), OVX+E2 ewes (samples from [Lomet et al](#)
150 [2018](#)) and OVX ewes (n=5 for May and n=4 for November; see **Fig S3A** for details). In
151 experiment 4, we used intact ewes of IdF (n=30) and Romanov (Rom; n=30) breeds. Ewes were

152 killed (n=10 per breed and time point) on February 13-16th, March 5-6th and March 15-16th, a
153 narrow seasonal time window during which anestrus develops in both breeds. The 1st two groups
154 (i.e. IdF and Rom breeds) were killed during a “natural” follicular phase (display of estrus behavior
155 when presented with a teaser ram). The remaining 40 ewes received a progestogen treatment
156 (vaginal sponge) on February 16-17th, which was removed on March 3-5th and followed by
157 pregnant mare serum gonadotropin (PMSG) injection. Ewes were killed 2 or 12 days later, when
158 displaying an “induced” follicular or luteal phase, respectively.

159

160 **RNA extraction and qRT-PCR analysis**

161 RNA extraction was performed on each MBH block using TriReagent (Sigma). Concentration and
162 purity of individual samples were determined with Nanodrop 2000 (ThermoScientific) and
163 integrity was checked by standard agarose gel electrophoresis. All procedures, including qPCR
164 assays for all target genes, have been thoroughly validated ([Lomet et al 2018](#); [Dardente and Lomet](#)
165 [2018](#)). cDNA was synthesised from each individual RNA sample using Omniscript RT kit
166 (Qiagen) and Oligo-dT primers (synthesized by Eurofins, Germany). The optimal cDNA dilution
167 and calibration curves for each PCR primer pair (Eurofins) were established using cDNA
168 synthesized from an equimolar mix of all individual RNA from each experiment. As a negative
169 control, the same mix with water instead of RT was prepared. Quantitative PCR (qPCR) was
170 performed using CFX-96 Real-Time PCR Detection System (Bio-Rad) and Sso Adv Universal
171 SYBR Green Supermix (Bio-Rad). All primer pairs had efficiencies ranging from 85% to 110%.
172 All samples (unknown, standard curves) were assessed in triplicate and Rplp0 (ribosomal subunit
173 P0, a.k.a 36B4) was used as a housekeeping gene. The quantification of mRNA level was obtained
174 by the $2^{-\Delta CT}$ method. Data are normalized and presented as fold-increase compared to the condition
175 with the lowest expression level. For Expt 4, all cDNA were re-synthesized in a single run to allow
176 direct comparison across conditions. The list of qPCR primers is provided in **Table S1**.

177

178 **In situ hybridization**

179 ISH was performed as described previously (Lomet et al 2018; Dardente et al 2019b).
180 Hypothalamic blocks for were cut into 20µm sections using a cryostat (CryoStar NX70,
181 ThermoScientific) and thaw-mounted onto SuperFrost Plus slides (ThermoScientific). Specific
182 probes were generated and validated (cloning & sequencing) as described above, using a mix of
183 MBH cDNA as template. Details of the inserts used to generate radioactive probes are provided in
184 **Table S1**. Radioactive cRNA riboprobes were prepared by plasmid linearisation and *in vitro*
185 transcription (Riboprobe System, Promega) including ³⁵S-UTP (Perkin-Elmer). Probes were
186 purified using Illustra Probe Quant G50 micro-columns (Fisher) and counted with a liquid
187 scintillation counter (Tri-Carb 2900TR, Packard). Slides were post-fixed at 4°C for 20 min in 4%
188 PFA, 0.1 M PB, rinsed with 0.1 M PB (2 X 5min), acetylated with 3.75% v/v of acetic anhydride
189 in 0.1 TEA, 0.05 N NaOH and finally rinsed with 0.1 M PB (2 X 5min). Slides were then
190 dehydrated through graded ethanol solutions (50%, 70%, 95% and 100%; 3min each) and dried
191 under vacuum for 60 min. Sections were hybridized overnight at 58°C with 10⁶ cpm of probe per
192 slide in hybridization buffer (50% deionized formamide, 10% dextran sulfate, 1 X Denhardt's
193 solution, 300 mM NaCl, 10 mM Tris, 10 mM DTT, 1 mM EDTA, 500 µg/mL tRNA). Sections
194 were then rinsed in 4 X SSC (3 X 5 min) and subjected to RNase-A digestion (20 µg/mL) in a
195 buffer containing 500 mM NaCl, 1 mM Tris, 1 mM EDTA for 30 min at 37°C. Stringency washes
196 in SSC (with 1mM DTT) were performed to remove non-specific probe hybridisation: 2 X SSC (2
197 X 5 min), 1 X SSC (10 min), 0.5 X SSC (10 min), 0.1 X SSC (30 min at 60°C), 0.1 X SSC (5 min).
198 Slides were then dehydrated through graded ethanol solutions, dried under vacuum for 60 min and
199 exposed to an autoradiographic film (BioMax MR, Kodak). Exposure duration was optimized for
200 each gene by repeated film exposures, depending on labeling intensity (from 3 days to 4 weeks).
201 Films were scanned on a transmittance image scanner (Amersham, UK) along with a calibrated

202 optical density (OD) transmission step wedge (Stouffer, USA). Calibrated Integrated OD (IOD)
203 measurements of gene expression within the MBH were performed using ImageJ software.

204

205 **Hormonal profile in OVX ewes**

206 Plasma levels of LH in OVX ewes (experiment 3) were assayed by RIA (Pelletier et al 1982). All
207 samples were included in a single assay and every sample was measured in duplicate. The assay
208 standard was 1051-CY-LH (equivalent to 0.31 NIH-LH-S1). Intra- and inter- assay coefficients of
209 variation averaged 9% and 15%, respectively with an assay sensitivity of 0.1 ng/mL.

210

211 **Data analysis**

212 Data were analysed using GraphPad Prism 6. ISH data were analysed by t-test (Mann-Whitney).
213 Data for qRT-PCR were analysed by one-way ANOVA (followed by post-hoc Tukey test when
214 applicable; Expts 2 and 4) or two-way ANOVA (Expt 3) using time (May and November) and
215 treatment (intact, OVX+E2 and OVX) as variables. The Sidak's post-hoc test was used for multiple
216 comparisons.

217

218 **Results**

219 We first used ISH to compare the seasonal expression pattern of candidate genes in the MBH of
220 intact ewes to the pattern we previously reported for OVX+E2 ewes (Lomet et al 2018; Dardente
221 and Lomet 2018). The PT markers *Tshb*, *Fam150b*, *Vmo1*, *Ezh2*, *Klkb1*, *Suv39H2*, *Vcan* and *Elovl6*
222 were expressed at higher levels in May than in November, while *Chga* and *Aa-Nat* showed the
223 opposite seasonal pattern, with higher expression in November than in May (Fig 1A & Fig S1, see
224 Table S2 for stats). The markers of tanycytes *Dio2*, *Tmem252*, *Shh* and *Slc01c1* showed increased
225 seasonal expression in May, while *NpSRI* was more expressed in November (Fig 1B). Therefore
226 we conclude that seasonal molecular markers of PT and tanycytes showed similar expression

227 patterns in intact and OVX+E2 ewes (Lomet et al 2018; Dardente and Lomet 2018),
228 notwithstanding possible differences in amplitude, which are difficult to assess from comparing
229 independent experiments.

230
231 This situation in PT and tanycytes differed markedly for the hypothalamic markers *Kiss1* and *Npvf*,
232 which did not display any difference in expression levels in intact ewes killed in May and
233 November (**Fig 1C**). This result is in stark contrast with what we found in OVX+E2 ewes, which
234 display *Kiss1* mRNA levels that are ~10-fold higher in November than in May, while *Npvf* displays
235 the opposite pattern with mRNA levels ~10-fold higher in May than in November (Lomet et al
236 2018).

237
238 We then used qRT-PCR to track seasonal changes of DEG in intact ewes with a more quantitative
239 approach and a finer temporal resolution (every 3 months). Seasonal high-amplitude rhythms of
240 expression were revealed for all PT markers (>50-fold for *Tshb*; **Fig 2A & Fig S2**, see **Table S2**
241 for stats) and for all tanycytic markers (>45-fold for *Tmem252*; **Fig 2A**, see **Table S2** for stats),
242 whether peak expression level occurs in May, or in November as in the case of *Chga* and *NpSRI*.
243 *Dio2* and *Dio3* displayed characteristic opposite patterns of seasonal expression, which predict
244 increasing and decreasing levels of T3 levels at the transition to anestrus and breeding, respectively
245 (deduced from the ratio *Dio2/Dio3*). Here again, expression levels for *Kiss1* and *Npvf* did not
246 display statistically significant seasonal rhythmicity (**Fig 2C** and **Table S2**).

247
248 To clarify the impact of E2 on molecular seasonal markers expressed in the three compartments
249 of the photoperiod transduction cascade – PT, tanycytes and hypothalamus – we employed OVX
250 ewes, and used qRT-PCR to allow a direct side-by-side comparison of relative expression levels
251 in May and November between intact, OVX+E2 and OVX ewes. Efficacy of OVX was validated

252 by RIA for LH (**Fig S3A**). Following removal of the E2 implant in March, LH levels increased
253 rapidly, reaching a plateau after 3-4 weeks. For the November group, LH levels had already
254 increased to their near-maximal level when the E2 implant was removed in August.

255
256 E2 was found to have little, if any, impact on the expression of the 9 PT markers investigated (**Fig**
257 **3A and Fig S3B**): all DEG showed high-amplitude rhythms in intact, OVX+E2 and OVX ewes
258 (2-way ANOVA, Time effect $p < 0.0001$ for all DEG; see **Table S2**).

259
260 A slightly different conclusion emerged for the 7 tanycytic markers (**Fig 3B and Fig S3C**). All
261 genes displayed statistically significant differences with time, even though the amplitude of the
262 rhythms appeared differentially affected across genes (2-way ANOVA, Time effect $p < 0.005$ for
263 all DEG; see **Table S2**). All May/Nov pairwise comparisons were statistically significant with
264 two exceptions: *Dio3* and *Shh* both displayed an increase in expression in OVX+E2 ewes, but
265 neither in intact nor in OVX ewes. Nevertheless, the *Dio2/Dio3* ratio remained higher in May for
266 all 3 groups of animals: 4.6-fold for OVX+E2, 2.8- and 3.2-fold for intact and OVX, respectively.

267
268 Consistent with our earlier findings using these samples from OVX+E2 ewes ([Lomet et al 2018](#)),
269 we found a ~10-fold increase in expression for *Kiss1* between May and November. Conversely,
270 *Npvf* expression decreased by ~10-fold between May and November. Most importantly, these large
271 opposite changes in *Kiss1* and *Npvf* expression were lost not only in intact ewes, but also in OVX
272 ewes see **Table S2** for stats). In intact ewes, *Kiss1* and *Npvf* levels were clamped to low and
273 intermediate-high levels, respectively. Conversely, in OVX ewes *Kiss1* and *Npvf* levels were
274 clamped to intermediate-high and low levels, respectively. Therefore, across the distinctive
275 experimental conditions, *Kiss1* and *Npvf* display inverse patterns of expression.

276

277 Intact and OVX+E2 ewes display roughly similar basal levels of E2 throughout the year
278 (Yuthasastrakosol et al 1975) but only intact ewes are further exposed to P4 during the breeding
279 season (Goodman & Inskeep 2015). We therefore went on to consider the importance of P4 for
280 the seasonal pattern of expression of *Kiss1* and *Npvf*, reasoning that the impact of cycling P4 might
281 somehow superimpose to the tonic E2-dependent photoperiodic impact on their expression level.

282
283 We attempted to get circuit-level insights on the potential impact of P4 by probing expression of
284 photoperiod-driven DEG in intact ewes at different phases of the estrous cycle (follicular vs luteal)
285 and during anestrus. As shown before (Fig 2) most DEG in PT and tanycytes show heightened
286 expression with increasing daylengths from February/March onwards, concomitant with anestrus
287 onset. We investigated a potential modulatory effect of P4 on DEG at this key transition, reasoning
288 that it might be easier to discern a modest impact in the course of photoperiodic induction. To do
289 so, we used a protocol in which expression of DEG was assessed on three occasions between mid-
290 February and mid-March and in two different ovine breeds, IdF and Rom. These breeds enter
291 estrus at the same time of year but anestrus occurs slightly later in Rom than in IdF ewes (Ben said
292 et al 2007). For the first two sampling points, ewes were in follicular phase, characterized by high
293 E2 levels and absence of P4, which allowed us to directly assess the impact of increasing
294 daylengths. The third group was killed 10 days after the second group, when ewes were in luteal
295 phase, characterized by high P4 and low E2. Results for the IdF and Rom breeds are shown in Fig
296 4A-C and Fig 4D-F, respectively (also see Fig S4 and Table S2 for stats).

297
298 The expression level of PT-specific DEG (Fig 4A & 4D), steadily increased (or decreased, *Chga*)
299 throughout the duration of the experiment, a trend which was more obvious in Rom compared to
300 IdF ewes. For example, expression of *Tshb* or *Fam150b* increased by ~3-4 fold in IdF ewes and
301 ~10-15 fold in Rom ewes. Therefore, P4 (Luteal, blue bars) does not appear to have any impact

302 upon photoperiodic induction or repression of PT-expressed DEG in either breed. As shown in
303 experiment 2 (see **Fig 2B**), PT and tanycyte DEG show almost synchronous and sustained increase
304 (or decrease) from February until May. In this paradigm, and contrasting with PT-expressed DEG,
305 the phase of the estrus cycle did appear to modulate the expression of DEG in tanycytes. Overall,
306 photoperiodic induction (or repression for *NpSRI*) of tanycytic DEG in the Luteal group were
307 typically reduced compared to those in the 2nd Follicular group (green bars) for IdF ewes (**Fig 4B**).
308 However, this decrease reached statistical significance only for *Tmem 252* and *Shh*. A very similar
309 trend was found for Rom ewes (**Fig 4E**), which displayed blunted induction (or decrease) of
310 tanycytic DEG when compared to PT markers. However, none of these markers displayed any
311 statistically significant differences between the 2nd and 3rd group of ewes. *Dio3* did not display any
312 significant changes in expression in either breed (data not shown). Finally, concomitant *Kiss1*
313 repression and *Npvf* induction in response to increasing daylengths were observed in both breeds
314 (**Fig 4C & Fig 4F**).

315

316 **Discussion**

317 Our analysis reveals the circuit-level logic of photoperiodic control of seasonal breeding (see
318 model, **Fig 5**). First, we show that seasonal rhythmicity of DEG in the PT is impervious to sex
319 steroids, which complements our earlier finding that these PT-expressed DEG are not impacted by
320 TH. These observations provide strong support for the hypothesis that the PT is a circannual timer.
321 Second, our analysis in IdF and Rom ewes at the transition towards anestrus point to a potential
322 role for P4 in modulating photoperiodic output at the level of tanycytes. Third, we demonstrate
323 that seasonal expression of *Kiss1* and *Npvf* is strongly modulated by sex steroids, with an intriguing
324 and consistent inverse relationship in their respective expression levels across experimental
325 conditions. Along with our prior finding that seasonal expression of *Kiss1* and *Npvf* is impacted
326 by the TH status ([Lomet et al 2018](#) ; see **Fig S5**), it places these two neuronal populations at the

327 crossroads between the photoperiodic input pathway and the sex steroid feedback. These findings
328 are most consistent with the notion that the “seasonal switch in the ability of E2 to inhibit the
329 GnRH pulse generator” occurs at the level of TH-responsive, *Kiss1*-expressing neurons of the
330 arcuate nucleus.

331
332 The possibility that the PT harbors the long sought-after circannual clock has now received strong
333 support from studies in sheep and hamsters ([Lincoln et al 2006](#) ; [Saenz de Miera et al 2013](#) ;
334 [Herwig et al 2013](#) ; [Saenz de Miera et al 2014](#) ; [Wood et al 2015](#) ; [Lomet et al 2018](#) ; [Dardente](#)
335 [2012](#) ; [Wood and Loudon 2018](#)). These studies demonstrated that expression of *Tshb* (and other
336 markers) in the PT displays long-term endogenous switches under a constant photoperiod, a
337 hallmark of a circannual clock. Similar changes were seen at the level of *Dio2/Dio3*, which are
338 presumably triggered through circannual changes in PT-TSH, even though the possibility that
339 tanycytes themselves harbor circannual clocks can not be ruled out ([Milesi et al 2017](#) ; [Lomet et](#)
340 [al 2018](#)). The circannual clock is predicted to be sheltered from cues other than melatonin in order
341 to consistently provide reliable timing information to downstream circuits.

342
343 We and others previously showed that gene expression in the PT is unresponsive to TRH and TH
344 ([Bockman et al 1997](#) ; [Dardente 2012](#) ; [Lomet et al 2018](#)). We now show that seasonal gene
345 expression in the PT is also unaffected by sex steroids. Therefore, neither TH nor E2, the two key
346 hormones in the progression of the seasonal breeding cycle, have any noticeable impact on
347 photoperiod decoding in the PT. We believe this is a strong argument in favor of the view that
348 melatonin-responsive PT-specific thyrotropes ([Klosen et al 2002](#) ; [Dardente et al 2003](#)) are indeed
349 circannual clocks. In this regard, a parallel between the PT and the SCN (master circadian clock)
350 may be drawn. The SCN is entrained by the light-dark cycle, while being insensitive to multiple
351 resetting cues including glucocorticoids ([Balsalobre et al 2000](#)), temperature ([Buhr et al 2010](#)) or

352 feeding schedule (Yamzaki et al 2000 ; Damiola et al 2000), which are all able to phase-shift
353 peripheral clocks (Dibner et al 2010 ; Mohawk et al 2012).

354
355 We show that P4 has a modest and gene-specific impact in tanycytes. Considering that tanycytes
356 receive photoperiodic information through PT-derived products (TSH and others ; Lomet et al
357 2018 ; Dardente et al 2019a), it leaves open the possibility that P4 somehow modulates the impact
358 of these entraining signal(s). Similar trends in gene expression patterns were seen in two different
359 ovine breeds (IdF and Rom) and for multiple molecular markers, which are either induced (*Dio2*,
360 *Tmem252*, *Shh*, *SlcO1c1*, *Dct*) or repressed (*NpSRI*) by lengthening photoperiods. We speculate
361 that functional relevance of this P4 feedback at the level of tanycytes, if any, may be more obvious
362 when the strength of the photoperiodic input is comparatively weak, which would correspond to
363 physiological transitions to anestrus or breeding. In the latter case, since P4 can not increase unless
364 ovulation occurs, P4 is unlikely to play any role in timing breeding onset. However, P4 may
365 modulate the timing of anestrus. However, we acknowledge that only *Tmem252* and *Shh* in IdF
366 ewes do show a statistically significant decrease upon P4 exposure. Once more, since OVX+E2
367 ewes undergo properly timed seasonal switches in LH/FSH, P4 is clearly dispensable for these
368 (Legan et al 1977). Therefore, great caution is required in the interpretation of the general trends
369 observed here, and the notion that P4 may exert a modulatory role will have to be tested further.

370
371 We notice that expression of *Shh* is affected by E2 (see **Fig 3B**) and P4 (in IdF ewes at least, see
372 **Fig 4A**), which implies that E2 and P4 impact upon tanycytes in a gene-specific manner. The
373 potential contribution of *Shh* to seasonal breeding through modulation of cell proliferation has
374 been discussed before (Dardente et al 2019 ; Dardente and Lomet 2019) ; the current finding that
375 E2 somehow modulates *Shh* suggests another layer of control. In sheep, the nuclear receptors ERα
376 and PGR are expressed in cells lining the third ventricle (Lehman et al 1993 ; Scott et al 2000).

377 Whether these cells are tanycytes is unknown, and co-localization with tanycyte-specific markers
378 would be required. In mouse, tanycytes appear to express ERa and PGR and display some
379 responses to P4 (Parkash et al 2015). However, a recent scRNAseq study failed to detect ERa or
380 PGR in murine tanycytes (Campbell et al 2017). Further experiments are required to clarify
381 expression of ERa and PGR in tanycytes and define whether they play any physiologically relevant
382 role. Considering the impact of tanycyte-derived T3 on the expression of *Kiss1* and *Npyf* in sheep
383 (Lomet et al 2018) and hamsters (Henson et al 2013 ; Klosen et al 2013), a potential role for sex
384 steroids in regulating DEG within tanycytes is of interest and warrants further investigation.

385
386 Amongst the DEG we characterized, *Kiss1* and *Npyf* are the only ones expressed by hypothalamic
387 neurons. *Kiss1* and *Npyf* are also the only DEG for which seasonal expression is abolished in both
388 intact and OVX ewes, compared to OVX+E2 ewes (Fig 1, Fig 2 & Fig 3). Therefore, seasonal
389 expression of these two genes is governed by photoperiod and sex steroids. There is strong
390 evidence that "final processes governing the onset of puberty in the lamb and the onset of the
391 annual season in the ewe share a common mechanism", based on a decrease in the ability of E2 to
392 inhibit the GnRH pulse generator (Legan et al 1977 ; Foster and Ryan 1979 ; Karsch et al 1984;
393 Goodman & Inskeep, 2015). In this respect, *Kiss1*-expressing neurons of the arcuate nuclei are
394 prime candidate (Beltramo et al 2014 ; Pinilla et al 2012 ; Simonneaux 2018).

395
396 We show that *Kiss1* is expressed at basal low levels throughout the year in intact ewes, which
397 contrasts with the large May/Nov difference seen in OVX+E2 ewes. While E2 is present at roughly
398 similar levels throughout the year in intact ewes, not overlooking the functionally critical but
399 modest 2-3 fold rise during the late follicular phase, P4 is produced exclusively during the breeding
400 season (Yuthasastrakosol et al 1975; Goodman & Inskeep 2015). Therefore, sex steroid status
401 during the anestrus season - presence of E2 and lack of P4 – can be considered similar in intact

402 and OVX+E2 ewes. This suggests that it is the presence of P4 during the breeding season, which
403 actively down-regulates the photoperiodic drive upon *Kiss1* expression. On the other hand, OVX
404 ewes display intermediate-to-high levels of *Kiss1* in both May and November, consistent with
405 prior findings (Pompolo et al 2006 ; Smith et al 2007 ; Smith et al 2008 ; Smith et al 2009 ;
406 Merkley et al 2012 ; Goodman & Inskeep, 2015). As assessed by c-Fos labeling, OVX is
407 accompanied by activation of KNDy neurons - but not of *Kiss1* neurons of the preoptic area -
408 which suggests that only *Kiss1* neurons in the arcuate nucleus are important for the E2 negative
409 feedback (Merkley et al 2012). Collectively, seasonal expression of *Kiss1* reflects E2-mediated
410 inhibition during anestrus, while E2-independent increase during the breeding season would be
411 masked by P4 inhibition during the luteal phase, and unmasked during the follicular phase. There
412 is prior evidence that both E2 and, to a lesser extent, P4 exert negative feedback on *Kiss1*
413 expression (Smith et al 2007 ; Smith et al 2008 ; Goodman et al 2011 ; Goodman & Inskeep, 2015).
414 We acknowledge that our experimental paradigm is not suitable to reveal a potential negative
415 impact of P4 upon *Kiss1* expression (**Fig 4**), which is decreasing at the transition towards anestrus
416 due to lengthening photoperiod.

417
418 Following a line of reasoning similar to the one developed above for *Kiss1*, we conclude that
419 seasonal expression of *Npvf* reflects E2-mediated activation during anestrus, while neither E2 nor
420 P4 impinge on *Npvf* expression during the breeding season. Consistent with our findings in intact
421 IdF ewes, we previously reported that photoperiod had little impact on *Npvf* expression in intact
422 Soay ewes (Dardente et al 2008). Furthermore, *Npvf* expression is not impacted by the transition
423 to long days in either intact Soay ewes (Dardente et al 2008) or OVX+E2 IdF ewes (Lomet et al
424 2018). Since such acute photoperiodic transition almost immediately impacts the gonadotropic
425 axis, we conclude that changes in *Npvf* transcription are not necessary for this physiological
426 response, a conclusion which holds true also for *Kiss1* (Lomet et al 2018). Interestingly, the

427 number of RFRP3-ir cells is 40% higher during the non-breeding season in OVX+E2 ewes (Smith
428 et al 2008). However, the expression level of *Npvf* was similar across breeding and non-breeding
429 seasons, in both OVX and OVX+E2 ewes (Smith et al 2008), which is not congruent with our
430 current findings. The reasons for this are unclear but may relate to the methods used (non-
431 radioactive ISH vs qRT-PCR).

432
433 Compared to KNDy neurons, the evidence for a direct control of *Npvf*-expressing neurons by sex
434 steroids is scarce (Goodman & Inskeep, 2015). In hamsters, about 40% of *Npvf* neurons express
435 ERa and E2 injection in OVX animals induces c-Fos in a subset of *Npvf* cells (Kriegsfeld et al
436 2006). In mouse, however, only 20-25% of *Npvf* neurons co-express ERa as assessed by ISH
437 (Molnar et al 2011 ; Poling et al 2012), while scRNAseq provides no evidence for co-expression
438 (Chen et al 2017). In sheep, we also found no evidence for co-expression (our unpublished
439 observations) while others reported that ~20% of *Npvf* neurons may express ERa (unpublished
440 observations, cited in Clarke & Arbabi 2016). These data are consistent with the overall distinct
441 distribution patterns of *Npvf*- (Dardente et al 2008) and ERa-expressing cells in the ovine MBH
442 (Lehman et al 1993 ; Blache et al 1994). *Npvf* neurons are most numerous at the level of the
443 VMH/DMH, where they tend to cluster medially, close to the third ventricle, while ERa-ir cells
444 are few at this level and rather scattered in lateral regions, farther from the third ventricle. In sheep,
445 the distribution of PGR does not provide support for co-expression with *Npvf*, since labeled nuclei
446 are not found in the DMH/VMH (Goubillon et al 2000 ; Dufourny and Skinner 2002 ; Smith et al
447 2007 ; Foradori et al 2002). These neuroanatomical considerations suggest that *Npvf*-expressing
448 neurons are not primary targets of sex steroids, even though the possibility that ERa/PGR are
449 expressed at low levels (i.e. below the detection threshold) can not be excluded.

450

451 Overall, the opposite expression patterns for *Kiss1* and *Npvf* in intact, OVX+E2 and OVX ewes
452 is striking. We suggest two non-mutually exclusive scenarios to explain this : sex steroids have
453 independent and opposite actions on both genes, or the two neuronal populations are somehow
454 connected such that the impact of sex steroids on one population leads to inhibition of
455 expression in the other. In both scenarios, the interplay between T3 and E2 is required to govern
456 proper seasonal timing (Lincoln and Short 1980 ; Karsch et al 1984 ; Karsch et al 1995 ;
457 Dardente 2012 ; Dardente et al 2014). The idea that *Npvf*-expressing neurons might be the
458 primary target for photoperiodic control has already been put forth in hamsters (Henningesen et
459 al 2016 ; Angelopoulou et al 2019). However, we deem this unlikely for several reasons. As
460 discussed above, KNDy cells do directly respond to sex steroids (presence of ER α and PGR)
461 and also contain the thyroid hormone receptor TR α (Dufourny et al 2016) ; they are therefore
462 well-placed to mediate the T3- and E2- dependent switches in seasonal breeding. Anatomically,
463 KNDy cells are also likely to receive contacts from beta-tanycytes processes, which traverse
464 the arcuate nucleus and reach the median eminence (Rodriguez et al 2005 ; Prévot et al 2018 ;
465 Rodriguez et al 2019). Indeed, KNDy cells might also receive signals, including T3, directly
466 from PT cells through the peculiar micro-vasculature of the arcuate nucleus region (Clarke
467 2015). Finally, the evidence that KISS1 is the key activator of reproduction in mammals is
468 overwhelming (Beltramo et al 2014 ; Pinilla et al 2012 ; Simonneaux 2018), while evidence
469 implicating RFRP3 is weak (Leon and Tena-Sempere 2016 ; Angelopoulou et al 2019).

470

471 In sheep, KISS1 and analogues consistently trigger GnRH/LH release and ovulation, even
472 during the anestrus season (Messenger et al 2005; Caraty et al 2007; Beltramo et al 2015; Decourt
473 et al 2016b; Beltramo & Decourt 2018). In comparison, we could not find any evidence for a
474 role of RFRP3 in GnRH/LH secretion (Decourt et al 2016a), which contrasts with earlier
475 findings (Clarke et al 2008). Genetic ablation of the RFRP3 receptor (NPFFR1) in mouse has

476 negligible impact upon reproduction (Leon et al 2014), while absence of KISS1R (a.k.a.
477 GPR54) leads to infertility (Messenger et al 2005; Pinilla et al 2012; Beltramo et al 2014).
478 Finally, there are only minimal projections from RFRP3 cells towards the arcuate nucleus,
479 which makes it unlikely that RFRP3 neurons make synaptic input onto KISS1 neurons in sheep
480 (Qi et al 2009). However, some evidence for such a unidirectional control has been found in
481 mouse (Poling et al 2013). Therefore, we can not exclude a primary role for *Npvf*-expressing
482 neurons in the seasonal response, but current evidence in sheep rather favor a model in which
483 these neurons are located downstream of KNDy neurons.

484
485 In conclusion our findings reveal the circuit-level logic of the impact of sex steroid of seasonal
486 breeding (Fig 5). The PT behaves as would be expected for a true circannual oscillator, sheltered
487 from the impact of sex steroids and TH, but acutely sensitive to photoperiod through melatonin.
488 Tanycytes display gene-specific regulation by both TH, E2 and P4, which we believe might help
489 fine-tune the timing for the onset and offset of the breeding season. Finally, neurons expressing
490 *Kiss1* emerge as a key node for the integration of environmental (photoperiod, through T3
491 responsiveness) and internal (feedback to sex steroid) cues, which together drive seasonal
492 breeding. Our analysis strongly suggests that *Kiss1* neurons of the arcuate nuclei are the cellular
493 substrate for the “seasonal switch in the ability of E2 to inhibit the GnRH pulse generator”. Finally
494 the opposite transcriptional control of *Kiss1* and *Npvf* expression over distinct states of sex steroid
495 feedback suggest some level of interconnection between these neuronal populations, the nature of
496 which remains to be identified.

497
498 **Figure legends**
499 **Figure 1** : Representative autoradiograms of *in situ* hybridization for a set of seasonal genes
500 expressed in the MBH of intact ewes in May and November : PT-expressed markers (black box),

501 tanycyte-specific markers (green box) and hypothalamic markers (red box). Note that all PT and
502 tanycyte markers display large seasonal variation in expression while *Kiss1* and *Npvf* show similar
503 expression levels in May and November (also see **Fig S1**).

504
505 **Figure 2** : qRT-PCR for a set of seasonal genes expressed in the MBH of intact ewes in November,
506 February, May and August : PT-expressed markers (black box), tanycyte-specific markers (green
507 box) and hypothalamic markers *Kiss1* and *Npvf* (red box). Note that all PT and tanycyte markers
508 display large seasonal variation in expression while *Kiss1* and *Npvf* show similar expression levels
509 in May and November (also see **Fig S2**).

510
511 **Figure 3** : Direct comparison of expression levels (as assessed by qRT-PCR) for a set of seasonal
512 genes expressed in the MBH of intact, OVX+E2 and OVX ewes in May and November. Note that
513 PT markers (black box) appear to be unaffected by the sex steroid status while some tanycyte
514 markers (green box) do show a moderate impact on amplitude (also see **Fig S3**). Also note that the
515 opposite May-Nov differences in expression seen for *Kiss1* and *Npvf* (red box) in OVX+E2 ewes
516 are lost in intact and OVX ewes. However, a consistent feature is the opposite pattern of expression
517 of both markers across the various sex steroid states.

518
519 **Figure 4** : qRT-PCR for a set of seasonal genes expressed in the MBH of intact ewes of the Ile-
520 de-France (panels A to C) and Romanov (panels D to F) breeds at the transition towards
521 anestrus (from mid February to mid March) : impact of P4. The length of the photoperiod at the 3
522 sampling times is superimposed to the *Tshb* data in panels A and D (red dots). Ewes were in
523 follicular phase for the first two sampling times and in luteal phase for the third sampling time.
524 Molecular markers in the PT (black box) and hypothalamus (red box) do show the expected
525 photoperiod-driven changes in expression in both breeds, with little (if any) overt impact of P4. In

526 contrast, photoperiod-driven changes in expression for tanycyte markers (green box) do seem to
527 be counterbalanced by P4 for both breeds (also see **Fig S4**).

528
529 **Figure 5** : A revised circuit-level model for the photoperiodic control of seasonal breeding (see
530 [Lomet et al 2018](#)). Here we show that sex steroids do not impact seasonal gene expression in the
531 PT. Together with prior findings that T3 does not have any effect either we conclude that the PT
532 is solely responsive to melatonin, which strengthens its role as a circannual clock. E2 and P4 may
533 have a modest and gene-specific impact upon seasonal gene expression in tanycyte, which could
534 play a modulatory role in timing the transition to anestrus. Finally, *Kiss1* and *Npvf* do show striking
535 opposite changes in expression under various sex steroid conditions, which suggest some form of
536 communication between these neuronal populations. Taking into account differential expression
537 of sex steroid receptors and neuroanatomical considerations, we favor a model in which *Kiss1* is
538 the target neuronal population of T3 and E2/P4 signaling in the control of seasonal breeding.

539

540

541 **Supplemental Materials**

542 Figures S1-S5

543 Table S1 : Word document

544 Table S2 : Excel file

545

546

547

548

549

550

551 Bibliography

- 552 Angelopoulou, E., Quignon, C., Kriegsfeld, L.J., et al., 2019. Functional Implications of RFRP-3 in the Central Control of Daily and Seasonal
553 Rhythms in Reproduction. *Front. Endocrinol. (Lausanne)* 10, 183.
- 554
- 555 Balsalobre, A., Brown, S.A., Marcacci, L., et al., 2000. Resetting of circadian time in peripheral tissues by glucocorticoid signaling. *Science* 289,
556 2344-2347.
- 557
- 558 Beltramo, M., Dardente, H., Cayla, X., et al., 2014. Cellular mechanisms and integrative timing of neuroendocrine control of GnRH secretion by
559 kisspeptin. *Mol. Cell. Endocrinol.* 382, 387-399.
- 560
- 561 Beltramo, M., Decourt, C., 2018. Towards new strategies to manage livestock reproduction using kisspeptin analogs. *Theriogenology* 112, 2-10.
- 562
- 563 Beltramo, M., Robert, V., Galibert, M., et al., 2015. Rational design of triazololipeptides analogs of kisspeptin inducing a long-lasting increase of
564 gonadotropins. *J. Med. Chem.* 58, 3459-3470.
- 565
- 566 Ben Said, S., Lomet, D., Chesneau, D., et al., 2007. Differential estradiol requirement for the induction of estrus behavior and the luteinizing hormone
567 surge in two breeds of sheep. *Biol. Reprod.* 76, 673-680.
- 568
- 569 Blache, D., Batailler, M., Fabre-Nys, C., 1994. Oestrogen receptors in the preoptico-hypothalamic continuum: immunohistochemical study of the
570 distribution and cell density during induced oestrous cycle in ovariectomized ewe. *J. Neuroendocrinol.* 6, 329-339.
- 571
- 572 Blache, D., Fabre-Nys, C.J., Venier, G., 1991. Ventromedial hypothalamus as a target for oestradiol action on proceptivity, receptivity and luteinizing
573 hormone surge of the ewe. *Brain Res.* 546, 241-249.
- 574
- 575 Bockmann, J., Bockers, T.M., Winter, C., et al., 1997. Thyrotropin expression in hypophyseal pars tuberalis-specific cells is 3,5,3'-triiodothyronine,
576 thyrotropin-releasing hormone, and pit-1 independent. *Endocrinology* 138, 1019-1028.
- 577
- 578 Buhr, E.D., Yoo, S.H., Takahashi, J.S., 2010. Temperature as a universal resetting cue for mammalian circadian oscillators. *Science* 330, 379-385.
- 579
- 580 Campbell, J.N., Macosko, E.Z., Fenselau, H., et al., 2017. A molecular census of arcuate hypothalamus and median eminence cell types. *Nat. Neurosci.*
581 20, 484-496.
- 582
- 583 Caraty, A., Fabre-Nys, C., Delaleu, B., et al., 1998. Evidence that the mediobasal hypothalamus is the primary site of action of estradiol in inducing
584 the preovulatory gonadotropin releasing hormone surge in the ewe. *Endocrinology* 139, 1752-1760.
- 585
- 586 Caraty, A., Lomet, D., Sebert, M.E., et al., 2013. Gonadotrophin-releasing hormone release into the hypophyseal portal blood of the ewe mirrors both
587 pulsatile and continuous intravenous infusion of kisspeptin: an insight into kisspeptin's mechanism of action. *J. Neuroendocrinol.* 25, 537-546.
- 588
- 589 Caraty, A., Smith, J.T., Lomet, D., et al., 2007. Kisspeptin synchronizes preovulatory surges in cyclical ewes and causes ovulation in seasonally
590 acyclic ewes. *Endocrinology* 148, 5258-5267.
- 591
- 592 Chen, R., Wu, X., Jiang, L., et al., 2017. Single-Cell RNA-Seq Reveals Hypothalamic Cell Diversity. *Cell. Rep.* 18, 3227-3241.
- 593
- 594 Clarke, I.J., 2015. Hypothalamus as an endocrine organ. *Compr. Physiol.* 5, 217-253.
- 595
- 596 Clarke, I.J., Arbabi, L., 2016. New concepts of the central control of reproduction, integrating influence of stress, metabolic state, and season. *Domest.*
597 *Anim. Endocrinol.* 56 Suppl, S165-79.
- 598
- 599 Clarke, I.J., Sari, I.P., Qi, Y., et al., 2008. Potent action of RFamide-related peptide-3 on pituitary gonadotropes indicative of a hypophysiotropic role
600 in the negative regulation of gonadotropin secretion. *Endocrinology* 149, 5811-5821.
- 601
- 602 Clarke, I.J., Smith, J.T., Caraty, A., et al., 2009. Kisspeptin and seasonality in sheep. *Peptides* 30, 154-163.
- 603
- 604 Damiola, F., Le Minh, N., Preitner, N., et al., 2000. Restricted feeding uncouples circadian oscillators in peripheral tissues from the central pacemaker
605 in the suprachiasmatic nucleus. *Genes Dev.* 14, 2950-2961.
- 606
- 607 Dardente, H., 2012. Melatonin-dependent timing of seasonal reproduction by the pars tuberalis: pivotal roles for long daylengths and thyroid
608 hormones. *J. Neuroendocrinol.* 24, 249-266.
- 609
- 610 Dardente, H., Birnie, M., Lincoln, G.A., et al., 2008. RFamide-related peptide and its cognate receptor in the sheep: cDNA cloning, mRNA distribution
611 in the hypothalamus and the effect of photoperiod. *J. Neuroendocrinol.* 20, 1252-1259.
- 612
- 613 Dardente, H., Hazlerigg, D.G., Ebling, F.J., 2014. Thyroid hormone and seasonal rhythmicity. *Front. Endocrinol. (Lausanne)* 5, 19.
- 614
- 615 Dardente, H., Klosien, P., Pevet, P., et al., 2003. MT1 melatonin receptor mRNA expressing cells in the pars tuberalis of the European hamster: effect
616 of photoperiod. *J. Neuroendocrinol.* 15, 778-786.
- 617
- 618 Dardente, H., Lomet, D., 2018. Photoperiod and thyroid hormone regulate expression of l-dopachrome tautomerase (Dct), a melanocyte stem-cell
619 marker, in tanycytes of the ovine hypothalamus. *J. Neuroendocrinol.* 30, e12640.
- 620
- 621 Dardente, H., Wood, S., Ebling, F., et al., 2019a. An integrative view of mammalian seasonal neuroendocrinology. *J. Neuroendocrinol.* 31, e12729.
- 622
- 623 Dardente, H., Lomet, D., Chesneau, D., et al., 2019b. Discontinuity in the molecular neuroendocrine response to increasing daylengths in Ile-de-
624 France ewes: Is transient Dio2 induction a key feature of circannual timing? *J. Neuroendocrinol.* 31, e12775.

625 Dardente, H., Wyse, C.A., Birnie, M.J., et al., 2010. A molecular switch for photoperiod responsiveness in mammals. *Curr. Biol.* 20, 2193-2198.
626
627 Decourt, C., Anger, K., Robert, V., et al., 2016a. No Evidence That RFamide-Related Peptide 3 Directly Modulates LH Secretion in the Ewe.
628 *Endocrinology* 157, 1566-1575.
629
630 Decourt, C., Robert, V., Anger, K., et al., 2016b. A synthetic kisspeptin analog that triggers ovulation and advances puberty. *Sci. Rep.* 6, 26908.
631
632 Dibner, C., Schibler, U., Albrecht, U., 2010. The mammalian circadian timing system: organization and coordination of central and peripheral clocks.
633 *Annu. Rev. Physiol.* 72, 517-549.
634
635 Dufourny, L., Gennetay, D., Martinet, S., et al., 2016. The Content of Thyroid Hormone Receptor alpha in Ewe Kisspeptin Neurones is not Season-
636 Dependent. *J. Neuroendocrinol.* 28, 12344.
637
638 Dufourny, L., Skinner, D.C., 2002. Progesterone receptor, estrogen receptor alpha, and the type II glucocorticoid receptor are coexpressed in the same
639 neurons of the ovine preoptic area and arcuate nucleus: a triple immunolabeling study. *Biol. Reprod.* 67, 1605-1612.
640
641 Foradori, C.D., Coolen, L.M., Fitzgerald, M.E., et al., 2002. Colocalization of progesterone receptors in parvicellular dynorphin neurons of the ovine
642 preoptic area and hypothalamus. *Endocrinology* 143, 4366-4374.
643
644 Foster, D.L., Ryan, K.D., 1979. Endocrine mechanisms governing transition into adulthood: a marked decrease in inhibitory feedback action of
645 estradiol on tonic secretion of luteinizing hormone in the lamb during puberty. *Endocrinology* 105, 896-904.
646
647 Franceschini, I., Lomet, D., Cateau, M., et al., 2006. Kisspeptin immunoreactive cells of the ovine preoptic area and arcuate nucleus co-express
648 estrogen receptor alpha. *Neurosci. Lett.* 401, 225-230.
649
650 Goodman, R.L., Holaskova, I., Nestor, C.C., et al., 2011. Evidence that the arcuate nucleus is an important site of progesterone negative feedback in
651 the ewe. *Endocrinology* 152, 3451-3460.
652
653 Goodman, R.L., Inskeep, E.K., Control of the ovarian cycle of the sheep. *Knobil and Neill's Physiology of Reproduction (Fourth Edition)* , 1259-
654 1305.
655
656 Goubillon, M.L., Forsdike, R.A., Robinson, J.E., et al., 2000. Identification of neurokinin B-expressing neurons as an highly estrogen-receptive,
657 sexually dimorphic cell group in the ovine arcuate nucleus. *Endocrinology* 141, 4218-4225.
658
659 Han, S.Y., McLennan, T., Czielesky, K., et al., 2015. Selective optogenetic activation of arcuate kisspeptin neurons generates pulsatile luteinizing
660 hormone secretion. *Proc. Natl. Acad. Sci. U. S. A.* 112, 13109-13114.
661
662 Hanon, E.A., Lincoln, G.A., Fustin, J.M., et al., 2008. Ancestral TSH mechanism signals summer in a photoperiodic mammal. *Curr. Biol.* 18, 1147-
663 1152.
664
665 Henningsen, J.B., Gauer, F., Simonneaux, V., 2016. RFRP Neurons - The Doorway to Understanding Seasonal Reproduction in Mammals. *Front.*
666 *Endocrinol. (Lausanne)* 7, 36.
667
668 Henson, J.R., Carter, S.N., Freeman, D.A., 2013. Exogenous T(3) elicits long day-like alterations in testis size and the RFamides Kisspeptin and
669 gonadotropin-inhibitory hormone in short-day Siberian hamsters. *J. Biol. Rhythms* 28, 193-200.
670
671 Herbison, A.E., 2018. The Gonadotropin-Releasing Hormone Pulse Generator. *Endocrinology* 159, 3723-3736.
672
673 Herwig, A., de Vries, E.M., Bolborea, M., et al., 2013. Hypothalamic ventricular ependymal thyroid hormone deiodinases are an important element
674 of circannual timing in the Siberian hamster (*Phodopus sungorus*). *PLoS One* 8, e62003.
675
676 Karsch, F.J., Bittman, E.L., Foster, D.L., et al., 1984. Neuroendocrine basis of seasonal reproduction. *Recent Prog. Horm. Res.* 40, 185-232.
677
678 Karsch, F.J., Dahl, G.E., Evans, N.P., et al., 1993. Seasonal changes in gonadotropin-releasing hormone secretion in the ewe: alteration in response to
679 the negative feedback action of estradiol. *Biol. Reprod.* 49, 1377-1383.
680
681 Karsch, F.J., Dahl, G.E., Hachigian, T.M., et al., 1995. Involvement of thyroid hormones in seasonal reproduction. *J. Reprod. Fertil. Suppl.* 49, 409-
682 422.
683
684 Klosen, P., Biennu, C., Demarteau, O., et al., 2002. The mt1 melatonin receptor and RORbeta receptor are co-localized in specific TSH-
685 immunoreactive cells in the pars tuberalis of the rat pituitary. *J. Histochem. Cytochem.* 50, 1647-1657.
686
687 Klosen, P., Sebert, M.E., Rasri, K., et al., 2013. TSH restores a summer phenotype in photoinhibited mammals via the RF-amides RFRP3 and
688 kisspeptin. *Faseb j.* 27, 2677-2686.
689
690 Kriegsfeld, L.J., Mei, D.F., Bentley, G.E., et al., 2006. Identification and characterization of a gonadotropin-inhibitory system in the brains of
691 mammals. *Proc. Natl. Acad. Sci. U. S. A.* 103, 2410-2415.
692
693 Legan, S.J., Karsch, F.J., Foster, D.L., 1977. The endocrin control of seasonal reproductive function in the ewe: a marked change in response to the
694 negative feedback action of estradiol on luteinizing hormone secretion. *Endocrinology* 101, 818-824.
695
696 Lehman, M.N., Coolen, L.M., Goodman, R.L., 2010. Minireview: kisspeptin/neurokinin B/dynorphin (KNDy) cells of the arcuate nucleus: a central
697 node in the control of gonadotropin-releasing hormone secretion. *Endocrinology* 151, 3479-3489.
698
699 Lehman, M.N., Ebling, F.J., Moenter, S.M., et al., 1993. Distribution of estrogen receptor-immunoreactive cells in the sheep brain. *Endocrinology*
700 133, 876-886.

701 Leon, S., Garcia-Galiano, D., Ruiz-Pino, F., et al., 2014. Physiological roles of gonadotropin-inhibitory hormone signaling in the control of
702 mammalian reproductive axis: studies in the NPF1 receptor null mouse. *Endocrinology* 155, 2953-2965.

703
704 Leon, S., Tena-Sempere, M., 2016. Dissecting the Roles of Gonadotropin-Inhibitory Hormone in Mammals: Studies Using Pharmacological Tools
705 and Genetically Modified Mouse Models. *Front. Endocrinol. (Lausanne)* 6, 189.

706
707 Lincoln, G.A., Clarke, I.J., Hut, R.A., et al., 2006. Characterizing a mammalian circannual pacemaker. *Science* 314, 1941-1944.

708
709 Lincoln, G.A., Short, R.V., 1980. Seasonal breeding: nature's contraceptive. *Recent Prog. Horm. Res.* 36, 1-52.

710
711 Lomet, D., Cognie, J., Chesneau, D., et al., 2018. The impact of thyroid hormone in seasonal breeding has a restricted transcriptional signature. *Cell*
712 *Mol. Life Sci.* 75, 905-919.

713
714 Merkley, C.M., Porter, K.L., Coolen, L.M., et al., 2012. KNDy (kisspeptin/neurokinin B/dynorphin) neurons are activated during both pulsatile and
715 surge secretion of LH in the ewe. *Endocrinology* 153, 5406-5414.

716
717 Messenger, S., Chatzidakis, E.E., Ma, D., et al., 2005. Kisspeptin directly stimulates gonadotropin-releasing hormone release via G protein-coupled
718 receptor 54. *Proc. Natl. Acad. Sci. U. S. A.* 102, 1761-1766.

719
720 Milesi, S., Simonneaux, V., Klosien, P., 2017. Downregulation of Deiodinase 3 is the earliest event in photoperiodic and photorefractory activation
721 of the gonadotropic axis in seasonal hamsters. *Sci. Rep.* 7, 17739-017-17920-y.

722
723 Mohawk, J.A., Green, C.B., Takahashi, J.S., 2012. Central and peripheral circadian clocks in mammals. *Annu. Rev. Neurosci.* 35, 445-462.

724
725 Molnar, C.S., Kalló, I., Liposits, Z., et al., 2011. Estradiol down-regulates RFamide-related peptide (RFRP) expression in the mouse hypothalamus.
726 *Endocrinology* 152, 1684-1690.

727
728 Moore, A.M., Coolen, L.M., Porter, D.T., et al., 2018. KNDy Cells Revisited. *Endocrinology* 159, 3219-3234.

729
730 Nakao, N., Ono, H., Yamamura, T., et al., 2008. Thyrotrophin in the pars tuberalis triggers photoperiodic response. *Nature* 452, 317-322.

731
732 Ono, H., Hoshino, Y., Yasuo, S., et al., 2008. Involvement of thyrotrophin in photoperiodic signal transduction in mice. *Proc. Natl. Acad. Sci. U. S.*
733 *A.* 105, 18238-18242.

734
735 Parkash, J., Messina, A., Langlet, F., et al., 2015. Semaphorin7A regulates neuroglial plasticity in the adult hypothalamic median eminence. *Nat.*
736 *Commun.* 6, 6385.

737
738 Pelletier, J., Garnier, D.H., de Reviers, M.M., et al., 1982. Seasonal variation in LH and testosterone release in rams of two breeds. *J. Reprod. Fert.*
739 64, 341-346.

740
741 Pinilla, L., Aguilar, E., Dieguez, C., et al., 2012. Kisspeptins and reproduction: physiological roles and regulatory mechanisms. *Physiol. Rev.* 92,
742 1235-1316.

743
744 Poling, M.C., Kim, J., Dhamija, S., et al., 2012. Development, sex steroid regulation, and phenotypic characterization of RFamide-related peptide
745 (Rfrp) gene expression and RFamide receptors in the mouse hypothalamus. *Endocrinology* 153, 1827-1840.

746
747 Poling, M.C., Quennell, J.H., Anderson, G.M., et al., 2013. Kisspeptin neurons do not directly signal to RFRP-3 neurons but RFRP-3 may directly
748 modulate a subset of hypothalamic kisspeptin cells in mice. *J. Neuroendocrinol.* 25, 876-886.

749
750 Pompolo, S., Pereira, A., Estrada, K.M., et al., 2006. Colocalization of kisspeptin and gonadotropin-releasing hormone in the ovine brain.
751 *Endocrinology* 147, 804-810.

752
753 Prevot, V., Dehouck, B., Sharif, A., et al., 2018. The Versatile Tanycyte: A Hypothalamic Integrator of Reproduction and Energy Metabolism. *Endocr.*
754 *Rev.* 39, 333-368.

755
756 Qi, Y., Oldfield, B.J., Clarke, I.J., 2009. Projections of RFamide-related peptide-3 neurons in the ovine hypothalamus, with special reference to
757 regions regulating energy balance and reproduction. *J. Neuroendocrinol.* 21, 690-697.

758
759 Rodriguez, E., Guerra, M., Peruzzo, B., et al., 2019. Tanycytes: A rich morphological history to underpin future molecular and physiological
760 investigations. *J. Neuroendocrinol.* 31, e12690.

761
762 Rodriguez, E.M., Blazquez, J.L., Pastor, F.E., et al., 2005. Hypothalamic tanycytes: a key component of brain-endocrine interaction. *Int. Rev. Cytol.*
763 247, 89-164.

764
765 Saenz de Miera, C., Hanon, E.A., Dardente, H., et al., 2013. Circannual variation in thyroid hormone deiodinases in a short-day breeder. *J.*
766 *Neuroendocrinol.* 25, 412-421.

767
768 Saenz de Miera, C., Monecke, S., Bartzen-Sprauer, J., et al., 2014. A circannual clock drives expression of genes central for seasonal reproduction.
769 *Curr. Biol.* 24, 1500-1506.

770
771 Scott, C.J., Pereira, A.M., Rawson, J.A., et al., 2000. The distribution of progesterone receptor immunoreactivity and mRNA in the preoptic area and
772 hypothalamus of the ewe: upregulation of progesterone receptor mRNA in the mediobasal hypothalamus by oestrogen. *J. Neuroendocrinol.* 12, 565-
773 575.

774
775 Simonneaux, V., 2020. A Kiss to drive rhythms in reproduction. *Eur. J. Neurosci.* 51, 509-530.

776

777 Smith, J.T., 2009. Sex steroid control of hypothalamic Kiss1 expression in sheep and rodents: comparative aspects. *Peptides* 30, 94-102.
778 Smith, J.T., Clay, C.M., Caraty, A., et al., 2007. KiSS-1 messenger ribonucleic acid expression in the hypothalamus of the ewe is regulated by sex
779 steroids and season. *Endocrinology* 148, 1150-1157.
780
781 Smith, J.T., Coolen, L.M., Kriegsfeld, L.J., et al., 2008. Variation in kisspeptin and RFamide-related peptide (RFRP) expression and terminal
782 connections to gonadotropin-releasing hormone neurons in the brain: a novel medium for seasonal breeding in the sheep. *Endocrinology* 149, 5770-
783 5782.
784
785 Smith, J.T., Li, Q., Pereira, A., et al., 2009. Kisspeptin neurons in the ovine arcuate nucleus and preoptic area are involved in the preovulatory
786 luteinizing hormone surge. *Endocrinology* 150, 5530-5538.
787
788 Urias-Castro, C., Arreguin-Arevalo, J.A., Magee, C., et al., 2019. Hypothalamic concentrations of kisspeptin and gonadotropin-releasing hormone
789 during the breeding season and non-breeding season in ewes. *Am. J. Reprod. Immunol.* 82, e13146.
790
791 Wagner, G.C., Johnston, J.D., Clarke, I.J., et al., 2008. Redefining the limits of day length responsiveness in a seasonal mammal. *Endocrinology* 149,
792 32-39.
793
794 Wood, S., Loudon, A., 2018. The pars tuberalis: The site of the circannual clock in mammals? *Gen. Comp. Endocrinol.* 258, 222-235.
795
796 Wood, S.H., Christian, H.C., Miedzinska, K., et al., 2015. Binary Switching of Calendar Cells in the Pituitary Defines the Phase of the Circannual
797 Cycle in Mammals. *Curr. Biol.* 25, 2651-2662.
798
799 Yamazaki, S., Numano, R., Abe, M., et al., 2000. Resetting central and peripheral circadian oscillators in transgenic rats. *Science* 288, 682-685.
800
801 Yuthasastrakosol, P., Palmer, W.M., Howland, B.E., 1975. Luteinizing hormone, oestrogen and progesterone levels in peripheral serum of anoestrous
802 and cyclic ewes as determined by radioimmunoassay. *J. Reprod. Fertil.* 43, 57-65.
803

804

805

□ May □ Nov

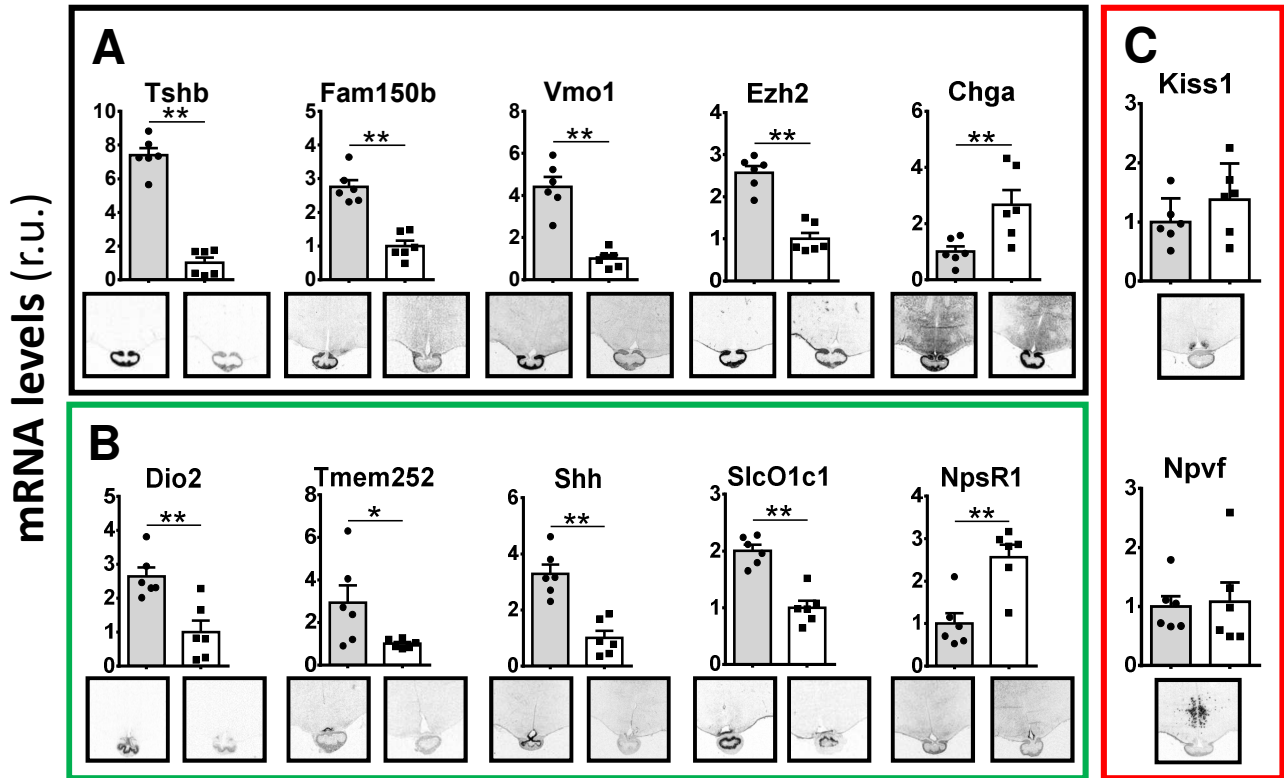


Fig.1
Intact ewes - ISH

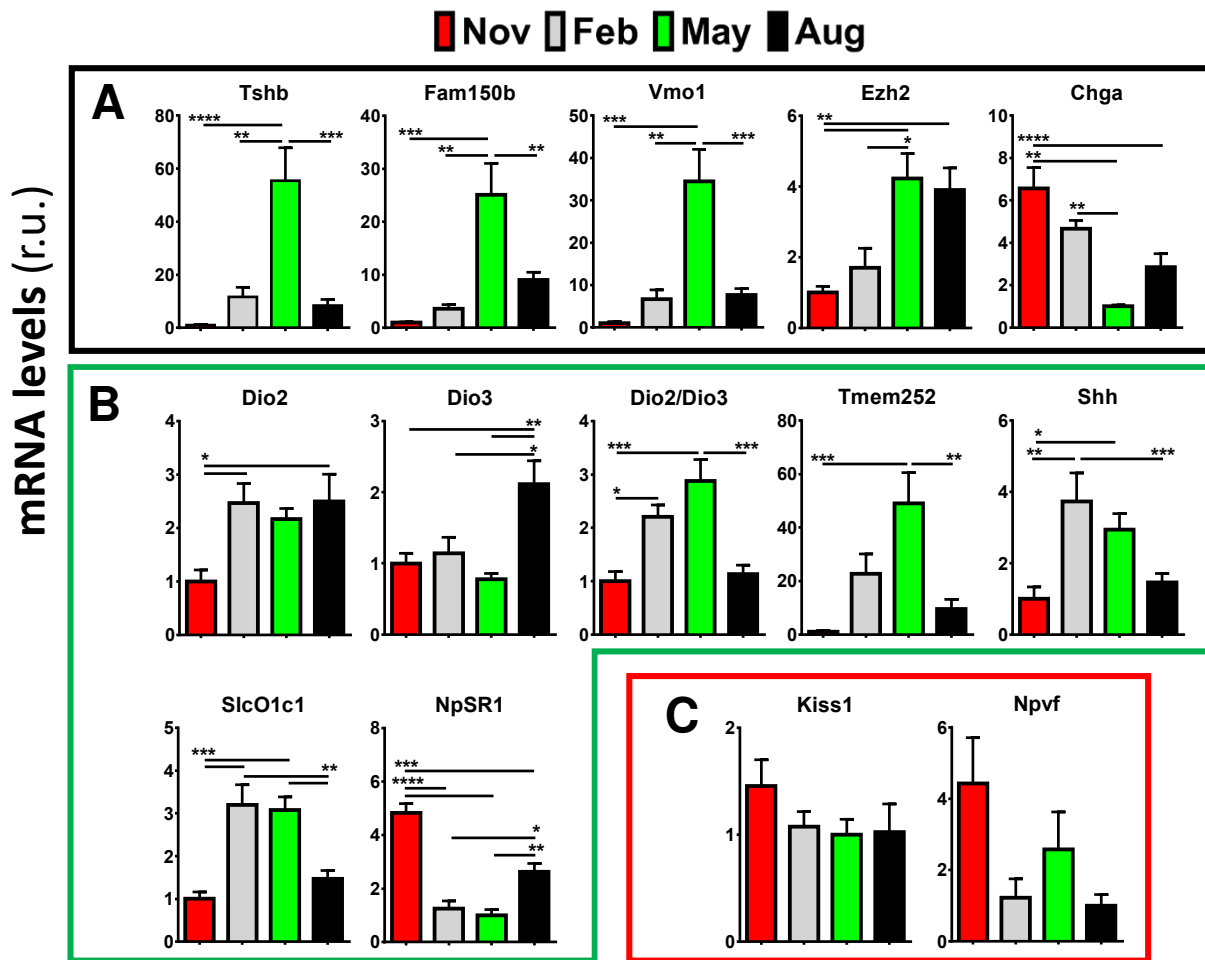


Fig.2
Intact ewes - qPCR

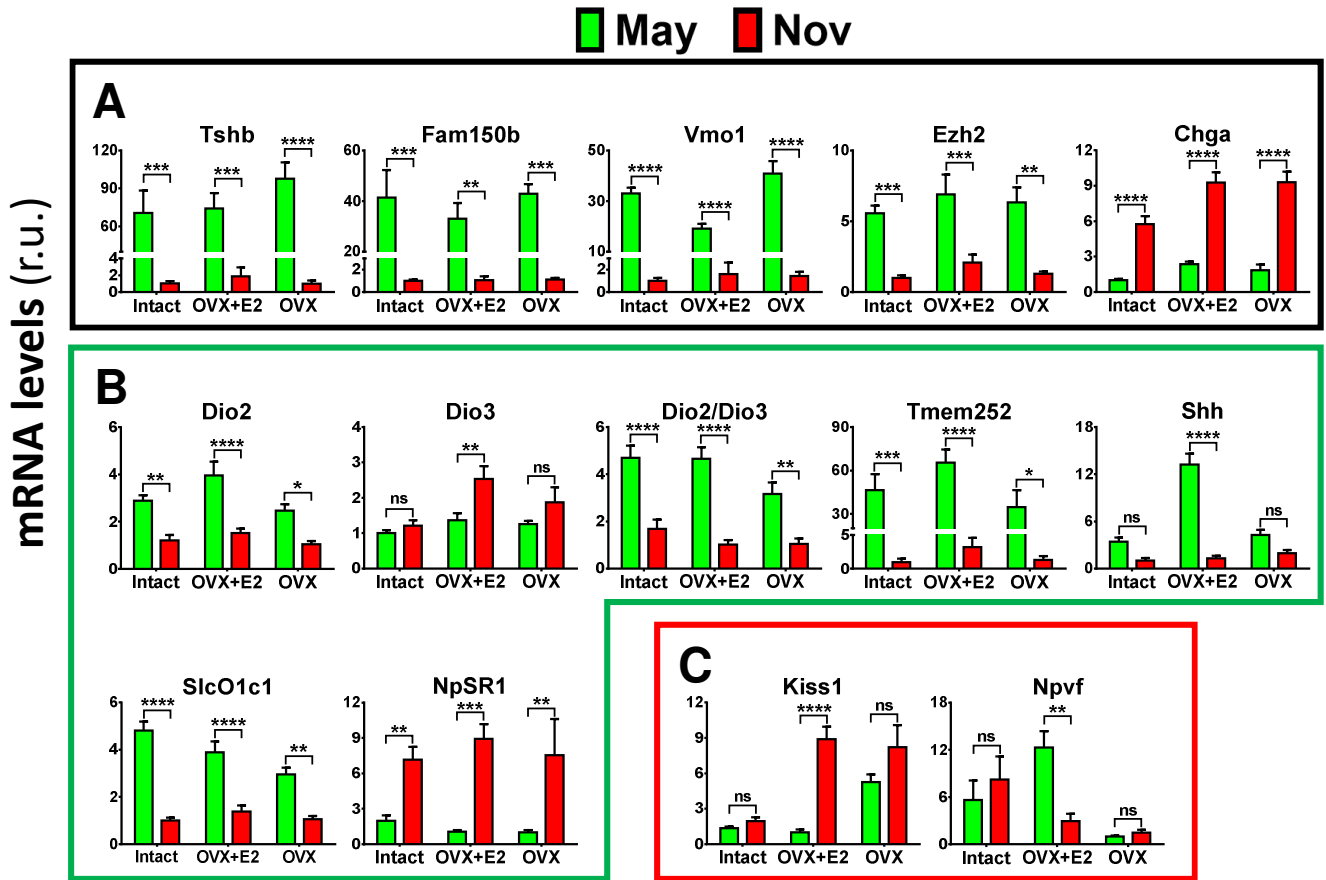


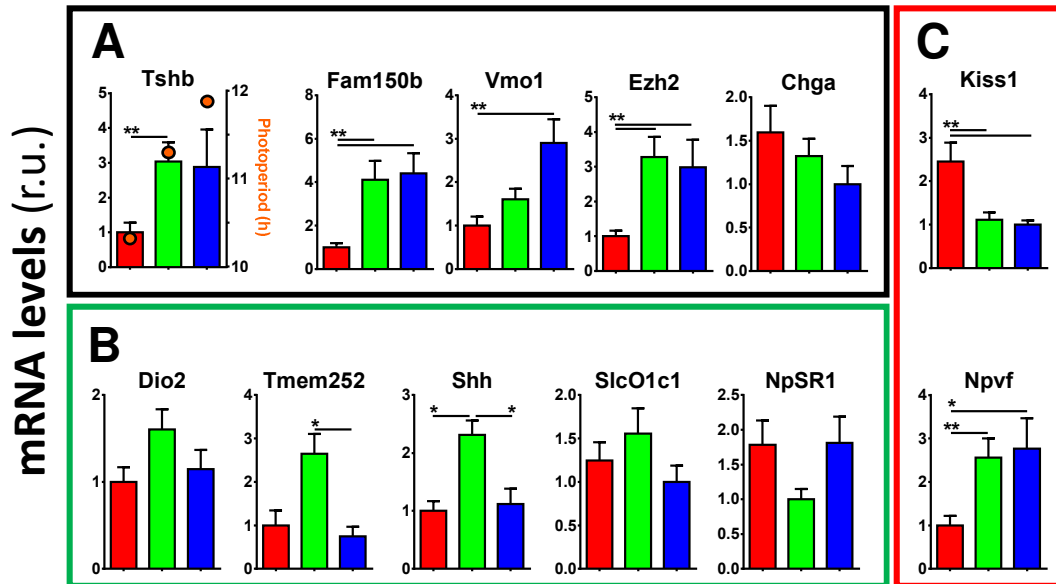
Fig.3
Intact VS OVX+E2 VS OVX

Ile-de-France

Follicular

Follicular

Luteal



Romanov

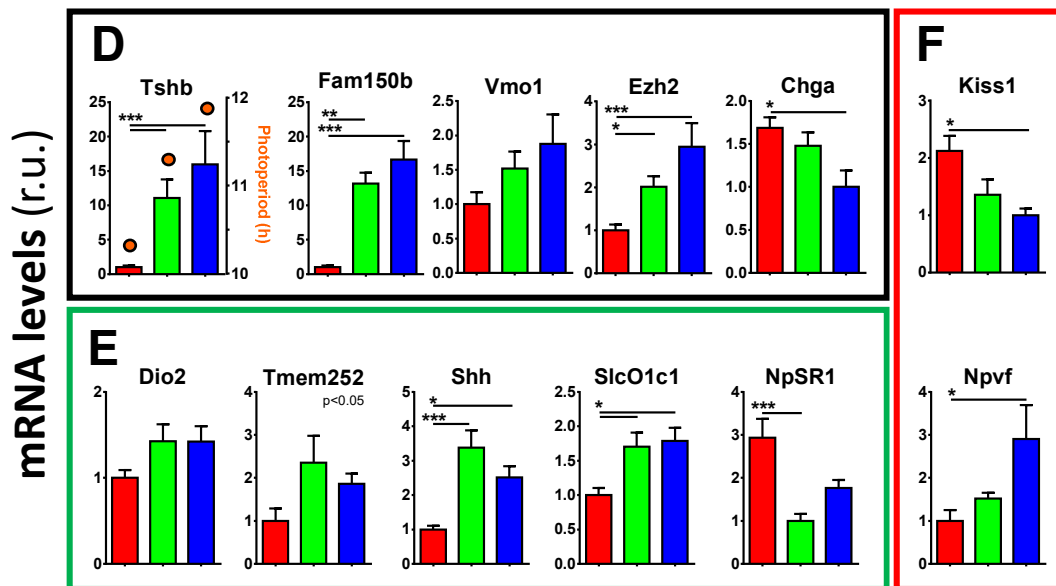


Fig.4
Pg VS Long PP

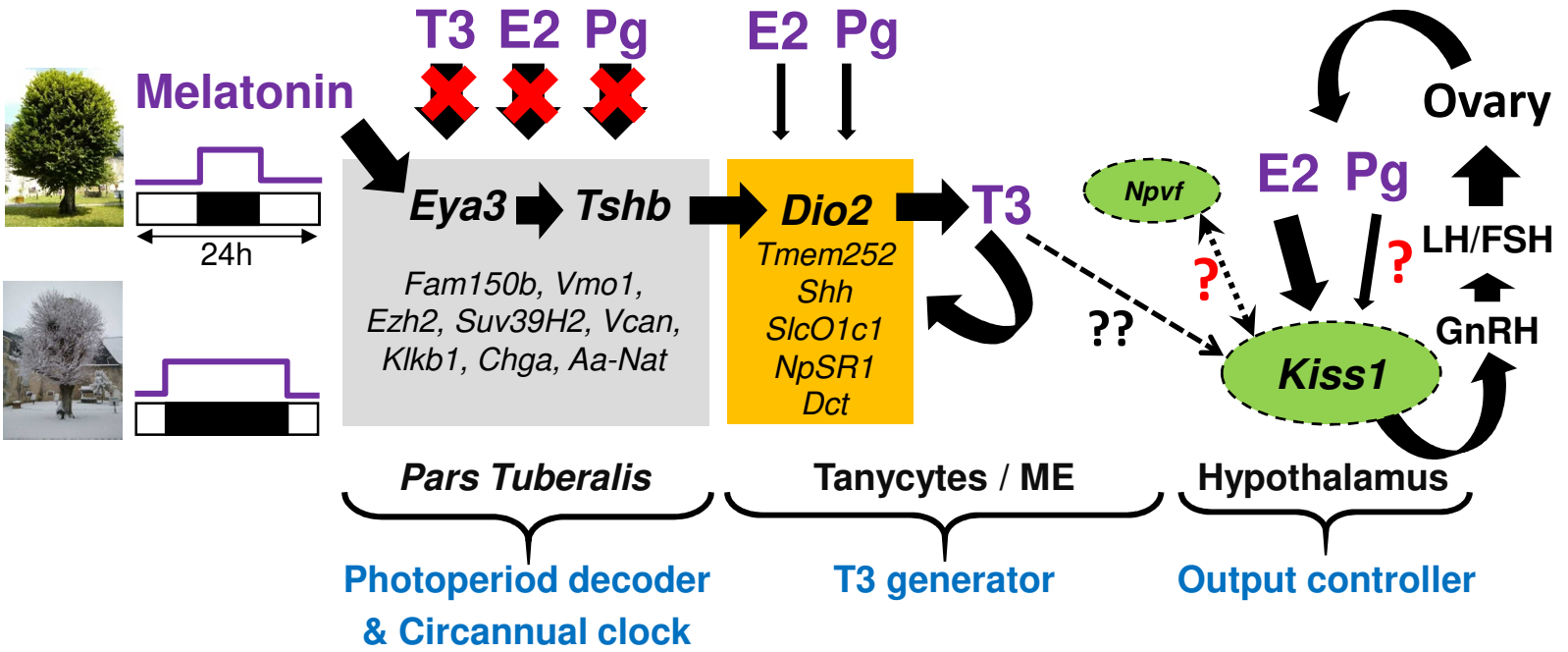


Fig.5
 General circuit-level model